Environmental Science & Technology

ARTICLE

pubs.acs.org/est

Dispersal and Attenuation of Trace Contaminants Downstream of the Ajka Bauxite Residue (Red Mud) Depository Failure, Hungary

William M. Mayes,*[,†] Adam P. Jarvis,[‡] Ian T. Burke,[§] Melanie Walton,[†] Viktória Feigl,[∥] Orsolya Klebercz,[∥] and Katalin Gruiz[∥]

[†]Centre for Environmental and Marine Sciences, University of Hull, Scarborough, YO11 3AZ, U.K.

[‡]School of Civil Engineering and Geosciences, Newcastle University, Newcastle upon Tyne, NE1 7RU, U.K.

[§]School of Earth and Environment, University of Leeds, Leeds, LS2 9JT, U.K.

[∥]Department of Applied Biotechnology and Food Science, Budapest University of Technology and Economics, 1111 Budapest, St. Gellért sq. 4, Hungary

Supporting Information

ABSTRACT: This paper identifies the spatial extent of bauxite processing residue (red mud)-derived contaminants and modes of transport within the Marcal and Rába river systems after the dike failure at Ajka, western Hungary. The geochemical signature of the red mud is apparent throughout the 3076 km^2 Marcal system principally with elevated Al, V, As, and Mo. Elevated concentrations of Cr, Ga, and Ni are also observed within 2 km of the source areas in aqueous and particulate phases where hyperalkalinity (pH < 13.1) is apparent. Although the concentrations of some trace elements exceed aquatic life standards in waters (e.g., V, As) and fluvial sediments (As, Cr, Ni, V), the spatial extent of these is limited to the Torna Creek and part of the upper Marcal. Source samples show a bimodal particle size distribution (peaks at 0.7 and 1.3 μm) which lends the material to ready fluvial transport. Where elevated concentrations are found in fluvial sediments, sequential extraction suggests the bulk of the As, Cr, Ni, and V are associated with residual (aqua-regia/HF digest) phases and unlikely to be mobile in the environment. However, at some depositional hotspots, association of As, Cr, and V with weak acid-extractable phases is observed.

INTRODUCTION

The dike breach at the bauxite processing residue (red mud) depository at the Ajkai Timfoldgyar Zrt alumina plant in Hungary on October 4, 2010 released between 600 000 and 700 000 m^3 of caustic red mud suspension.[1] Although there have been other notable examples of accidental release of caustic wastes to river systems,[2,3] the Ajka incident is unprecedented given the scale of the release and the type of material involved. Immediate scientific efforts at the site have assessed the phytotoxicty of the red mud given the vast areas (estimated to be 800 ha)[4] of agricultural land inundated and the public health risks associated with dust blows from the terrestrial deposits.[5,6]

Red mud is the fine fraction byproduct of alumina refining, of which between 70 million and 120 million tonnes are produced annually.[4,7,8] The specific composition of red mud deposits, and their trace element constituent in particular, depends on the quality of the bauxite ore from which they are enriched in the residue. The bulk matrix of red mud typically comprises residual iron oxides (e.g., hematite), quartz, sodium aluminosilicates, titanium dioxide, calcium carbonate/aluminate, and sodium hydroxide (which elevates pH up to 13).[5,9] At Ajka, previous studies have highlighted the presence of radionuclides (^{226}Ra, ^{232}Th, and ^{40}K) in the deposits[7] and characterization studies soon after the spill highlighted elevated concentrations of V, Cr, Ni, and Co in two isolated red mud samples taken from deposits downstream of the site.[4] Immediate studies on the bioavailability of potential trace contaminants to plants suggest that trace contaminant availability (e.g., Cr, Co, Ni, and V) is a secondary issue compared to an elevated Na content of the material.[4] These findings are consistent with other assessments undertaken on red mud deposits from sites elsewhere globally[10] suggesting that the material, while enriched in various trace elements, can be relatively benign. Indeed, multiple after-uses for red mud have been assessed in building materials[7] and as an environmental ameliorant.[11] Red mud and derivative media have been shown to limit the mobility of many trace contaminants in various contaminated land settings (e.g., mine sites) due primarily to sorption and coprecipitation with the abundant ferric and aluminum oxides in the material.[12−14]

Red mud leachates are hyperalkaline (pH 9−13) due to the NaOH digestant used in the Bayer Process.[15] High pH itself in surface waters can be a source of direct toxicity to aquatic life.[16]

Received: March 26, 2011
Accepted: May 6, 2011
Revised: May 4, 2011
Published: May 18, 2011

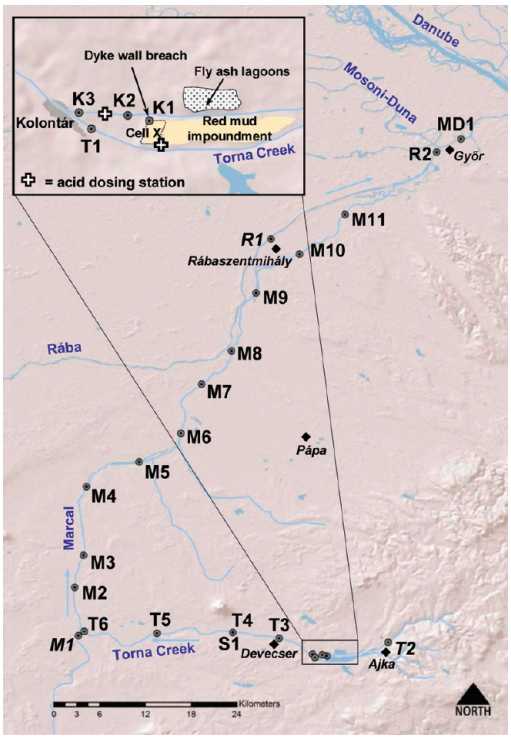

Figure 1. Location map of sample stations (circles). Centers of population shown with diamonds. Reference site labels in italics.

However, an equally important issue is the greater mobility of oxyanionic trace elements such as As, Cr, Mo, and V at elevated pH.[17] These contaminants have been documented to occur in concentrations of 2−5 mg L^{-1} at a former mine pit lake in which red mud was dumped in western Poland.[15] Studies in analogous hyperalkaline settings have also documented some of these elements occurring at environmentally significant concentrations, such as in waters draining steel slag mounds,[18] chromite ore residue sites,[19] and fly ash disposal sites.[20]

This paper presents an integrated assessment of water quality, contaminant transport and fate in the water courses immediately downstream of the Ajka red mud disposal site. Specific objectives of the work are to (1) assess the impact, composition, and behavior of residual aqueous releases from the disposal site, and (2) determine the spatial extent and form of red mud-derived contaminants in the fluvial sediments downstream of the site.

EXPERIMENTAL SECTION

Study Site. Sample locations along the course of the Torna Creek, Marcal, Rába, and Mosoni-Duna rivers are shown in Figure 1. Land cover across the catchments is dominated by agriculture, with principal urban areas at Ajka, Pápa, and toward the confluence with the Mosoni-Duna around the town of Győr. Bedrock geology in the upper catchment is dominated by dolomites and limestones of Triassic age which lie beneath a sequence of fluvial marls, slates, and interbedded sands of Miocene age.[1] The Torna, Marcal, and Rába are all extensively channelized with levees minimizing floodplain extent, particularly downstream of Pápa (Figure 1).

Water Analyses. Water and sediment samples were collected from the locations shown in Figure 1 under consistent low-to-moderate winter flow conditions on December 1 and 2, 2010 (mean daily flow at M4 was 11.5 $m^3 s^{-1}$ on both days). Field data and water samples were collected according to standard sampling protocols (see Supporting Information). Major anion concentrations were determined using a Dionex 100 ion chromatograph and cation and minor element concentrations were determined using a Perkin-Elmer Elan DRCII inductively coupled plasma−mass spectrometer (ICP-MS; for As, Cr, and Mo) and an Optima 5300 DV ICP-OES for all other elements quoted hereafter.

Sediment Samples. At each station triplicate bulk (≈ 500 g) sediment samples were collected by aggregating three randomly collected subsamples from a 12 m^2 area of stream bed (9 separate locations sampled at each reach to give three replicates). Additional spot samples of transported red mud from floodplain deposits at Somlóvásárhely (S1), fly ash (that formed the disposal cell wall), stock-piled gypsum (used to dose waters in the spill aftermath), and gypsum-affected fluvial sediments were taken at selected sites. Sediments were homogenized, air-dried, disaggregated gently, and sieved (2 mm aperture) prior to microwave-assisted total digestion (aqua regia and HF) following standard methods.[21] Elemental concentrations in digests were analyzed as per aqueous trace element analyses. Selected dried and disaggregated samples from K1 and S1 were also prepared for SEM/EDS and particle size analysis. Sequential extraction on combined triplicate samples from the sample stations was undertaken to increase extractant solution/sediment ratio.[22] Extractant pH was checked after each stage and conformed to standard values. All statistical analyses were undertaken in Minitab v15. Data were not normally distributed even after log-transformation (Kolmogorov−Smirnov $p > 0.05$) so nonparametric methods were used. Principal Component Analysis (PCA) was undertaken on standardized sediment element concentration data.

RESULTS AND DISCUSSION

Major Ion Chemistry. Reference samples (T2, M1) across the upper catchment are similar in composition, being slightly alkaline, dominated by Ca−Mg−HCO_3 type, consistent with waters draining from the Triassic dolomites (Table 1). Waters at site K1 characterize those draining Cell X (Figure 1), which was the active cell at the western-most end of the disposal site and contained fine-grained bauxite residue (red mud).[1] The K1 waters characterize the leachate and red mud suspension preacid dosing, and show Na−CO_3−OH dominated waters with hyperalkaline pH (13.1), low *Eh*, high suspended solid content (13.3 g L^{-1}), and high SO_4^{2-} concentrations. The K1 site lies at the base of a permeable reactive fly ash barrier (constructed using material from the dam wall), built within 2 weeks of the accident across the dike breach. Downstream of K1 the waters are directed through a series of settlement lagoons and acid dosing units (HCl and H_2SO_4) prior to the confluence of the northerly branch of the Torna Creek with its southerly branch (Figure 1). The decrease in pH between K1 and K2 is explicable by dilution of the waters from Cell X with uncontaminated waters on the northern branch of the Torna Creek. Lagoons and check dams shortly downstream of K1 appear effective in substantially reducing the suspended solid content of the water, while further decreases in pH are apparent downstream (K3) due to acid dosing (Table 1). While the drainage from K1 represents a significant point source of hyperalkaline leachate to surface waters around the site, there are additional inputs of leachate from Cell X into the southerly branch of the Torna Creek

Table 1. Hydrochemical Composition of the Waters in the Torna Creek and Upper Marcal on December 1, 2010[a]

determinand	T2	K1	K2	K3	T1	T3	T4	T5	T6	M1
pH	8.30	13.06	10.50	10.08	8.40	8.34	8.46	8.71	8.60	8.31
temperature (°C)	2.8	3.6	4.2	3.9	5	3.3	2.6	1.3	1.6	0.7
specific conductance (μS cm^{-2})	825	162900	3597	1715	1448	1505	1175	1076	966	911
ORP (V)	0.125	0.023	0.057	0.003	0.033	0.054	0.040	0.038	0.111	0.106
mean velocity (m s^{-1})	0.81	<0.01	0.76	0.21	1.27	1.70	1.04	0.90	0.65	-
major ions/elements mg L^{-1}										
Ca	143 (138)	1515 (1.3)	89.13 (16.86)	37.50 (15.21)	213.08 (198.99)	184.91 (175.02)	169.30 (161.52)	140.51 (134.22)	136.76 (132.91)	121.31 (120.80)
Mg	37 (36)	9.7 (0.001)	21.92 (13.29)	12.48 (9.02)	53.11 (50.58)	45.52 (44.56)	39.45 (39.07)	38.78 (38.38)	36.62 (36.39)	41.27 (41.36)
K	5 (5)	115 (85)	35.24 (35.60)	35.14 (35.24)	8.33 (8.04)	11.10 (11.39)	8.45 (8.43)	8.68 (8.64)	7.25 (7.15)	7.55 (7.69)
Na	13 (12)	(701)	374.15 (369.12)	393.90 (392.73)	68.42 (67.25)	139.38 (137.57)	79.10 (78.37)	79.59 (79.10)	52.85 (52.14)	24.30 (24.34)
Al	0.2 (0.01)	1228 (659)	18.19 (11.63)	12.73 (9.02)	9.96 (0.25)	9.83 (0.37)	4.01 (0.41)	3.75 (0.64)	1.88 (0.23)	0.22 (0.04)
Cl	25	83	49.70	116	34.60	110	50.90	47.20	37	31.20
SO_4	67	727	283	260	363	321	256	185	154	97.40
total alkalinity	340	7160	570	440	342	334	300	348 (316)	298 (296)	346 (340)
OH calculated		1125.8	1.10							
CO_3 calculated		2445.8	248							
HCO_3 calculated	414.80	1.40	165.20	536.80	417.24	407.48	366.00	424.56	363.56	422.12
suspended solids	49.6	13260	490.0	208.0	139.6	105.6	82.0	87.6	70.8	0.4
trace elements (μg L^{-1})										
As	<0.1	3926 (3612)	224 (156)	181 (147)	108 (29)	124 (1)	43 (4)	37 (4)	33 (4)	<0.1
B	<2	1009 (900)	30 (30)	<2	<2	<2	<2	<2	<2	<2
Ba	50 (46)	297 (1)	34 (3)	14 (3)	45 (33)	39 (23)	39 (27)	39 (27)	41 (33)	47 (45)
Be	<0.1	46 (<0.1)	<0.1	<0.1	<0.1	<0.1	<0.1	<0.1	<0.1	<0.1
Cd	<0.1	59 (53)	3 (<0.1)	<0.1	<0.1	2 (<0.1)	<0.1	<0.1	<0.1	<0.1
Co	<1	17 (<1)	<1	<1	<1	<1	<1	<1	<1	<1
Cr	<0.1	356 (49)	1.2 (0.9)	5.8 (4.5)	8.7 (5.6)	6.6 (4.3)	1.4 (<0.1)	4.6 (<0.1)	1.0 (<0.1)	<0.1
Cu	3 (2)	390 (310)	15 (9)	18 (14)	5 (2)	5 (3)	4 (2)	4 (2)	3 (2)	2 (2)
Fe	346 (<10)	10212 (<10)	1080 (<10)	610 (<10)	760 (<10)	380 (<10)	360 (<10)	430 (<10)	500 (<10)	150 (<10)
Ga	12 (11)	2350 (2340)	129 (120)	122 (117)	79 (31)	72 (39)	47 (35)	40 (37)	22 (19)	18 (<1)
Li	4 (4)	303 (27)	215 (213)	197 (197)	22 (19)	37 (36)	20 (20)	20 (18)	13 (13)	8 (7)
Mn	84 (39)	9894 (<1)	130 (3)	77 (8)	208 (67)	205 (87)	161 (81)	175 (86)	210 (86)	29 (20)
Mo	19 (11)	5443 (4114)	405 (398)	420 (416)	77 (74)	155 (152)	83 (78)	93 (77)	58(44)	13 (11)
Ni	5 (<1)	267 (36)	6.7 (4.5)	6.9 (4.6)	9.0 (6.0)	8.6 (6.1)	7.6 (5.9)	8.6 (4.5)	9.1 (5.8)	1.8 (1.4)
Pb	12 (2)	<1	0.00 (0.01)	<1	<1	<1	2 (<1)	7 (<1)	4 (<1)	<1
Si	3389 (3211)	499248 (668)	4473 (1524)	2635 (1044)	3808 (2885)	3644 (2588)	3077 (2110)	3062 (2052)	3206 (2609)	3099 (2884)
Sr	251 (241)	8819 (2)	334 (153)	165 (107)	909 (848)	755 (711)	582 (557)	553 (528)	512 (500)	509 (499)
V	<1	6398 (5709)	334 (323)	347 (343)	66 (26)	103 (60)	48 (39)	47 (41)	35 (30)	<1
W	<5	510(483)	19 (10)	19 (9)	<5	<5	<5	<5	<5	<5
Zn	13 (10)	446 (49)	20 (2)	8 (1)	27 (14)	21 (16)	23 (13)	16 (10)	13 (10)	21 (19)

[a] Data present total values with filtered (0.45μm filter) data in parentheses. '<' denotes values below the given limit of detection.

dx.doi.org/10.1021/es200850y |Environ. Sci. Technol. 2011, 45, 5147–5155

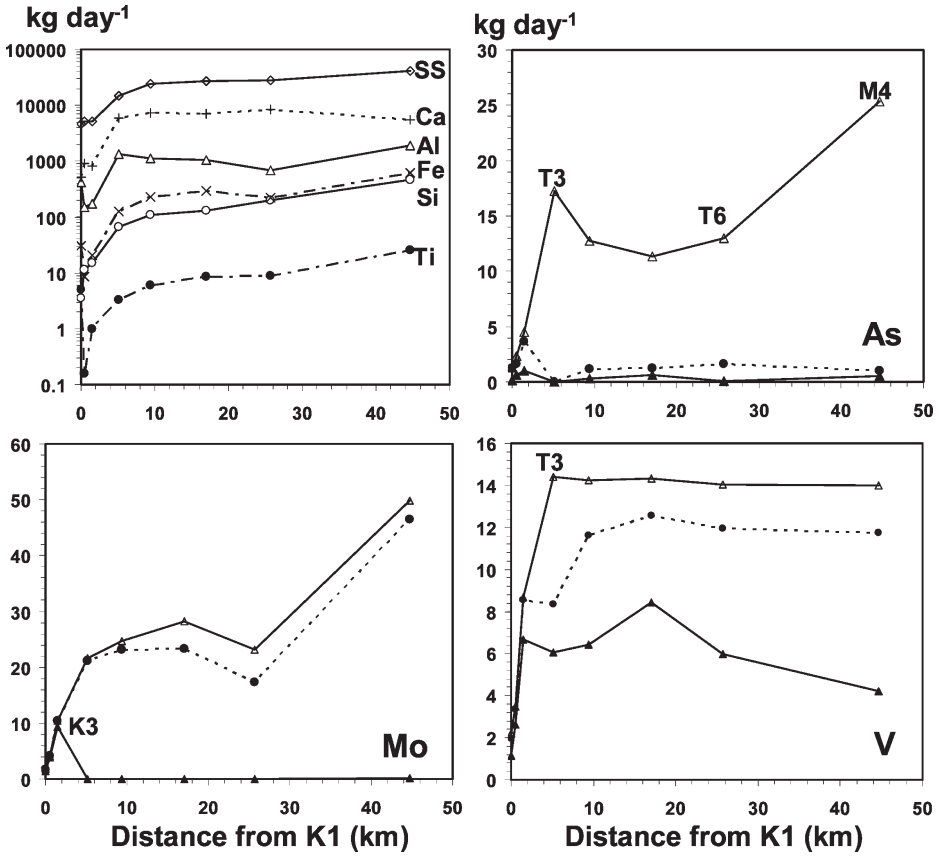

Figure 2. Partitioning of load (kg day^{-1}) of selected metals and metalloids with distance downstream of the dike breach alongside suspended solid loading (kg day^{-1}). Particulate loading for major elements only shown in upper left image alongside suspended solids (SS). Note also logarithmic *y* axis on upper left image. All other images show total loading (Δ marker with solid black line), filtered (0.45 μm) loading (● marker with dashed black line), and dissolved (passes 10 kDa centrifuge filter) loading (▲ marker with solid black line).

(just upstream of T1) via an acid dosing unit (reflected in SO_4^{2-} elevations above reference sites) to the south of Cell X. The dilution of the contaminated water with progress downstream is reflected in monotonic decrease in Na^+ and SO_4^{2-} toward baseline concentrations, which are achieved toward the confluence of the Rába and the Mosoni-Duna.

Major and Trace Elements. In hyperalkaline conditions at K1 numerous trace elements are elevated in both the particulate and dissolved phase. Dissolved concentrations of Al, As, Cr, Ga, Mo, Ni, Se, V, and U (Table 1) are similar to those documented elsewhere.[15] Soluble oxy(anionic) species are generally only detected in the northern branch of the Torna Creek where pH remains elevated prior to acid dosing (Table 1, Figure S1) and subsequent dilution at T1−T3. Cr, Ni, Se, and U concentrations decrease to baseline (similar to reference site) levels or below detection limits by K3, due to changing solubility with the decrease in pH (from 13.1 to 10.1)[17] and dilution. The trace elements for which elevated concentrations in the water column are seen to propagate furthest downstream are As, Mo, and V (Table 1, Figure S1). These form oxyanions in moderate to highly alkaline conditions and are a well-documented water quality issue in waters draining high pH industrial residues.[20,23] In the circum-neutral pH, oxic conditions downstream of K3, arsenic would be expected to be immobilized by sorption or coprecipitation with both hydrous ferric oxide (HFO) and oxides of Al[24,25]for which numerous phases are predicted to be oversaturated around source areas. Mass loading data highlight such rapid attenuation of dissolved As between K3 and T3. Arsenic shows significant ($p < 0.05$) positive correlation with particulate Al, Ca, and Ti ($r_s = 0.49-0.54$) and no significant ($p < 0.05$) correlation with Fe, which may be a feature of consistently high Fe concentrations throughout the system from both Ajka and natural lithogeneous sources.

At the water pH values measured the element V is predicted to be present principally as vanadate (VO_4^{3-})[26] and analysis of fractions within the water column via sequential filtration highlight a significant portion of V (typically 51−77%) being transported in the dissolved phase around the source areas (K1−T3; Figure 2). The total loading of V (Figure 2) stays relatively constant throughout the lower Torna and into the Marcal. However, the proportion of particulate and colloidal V in particular becomes more important with distance down the Torna, suggesting sorption and/or (co)precipitation of dissolved V (Figure 2). There are strong and significant ($p < 0.001$) correlations between particulate V and all major particulate vectors (Al, Ca, Fe, Si, Ti; $r_s = 0.76-0.92$) alluding to their importance in V attenuation and transport.[27,28] The total V concentrations exceed recommended freshwater EQS[29] at the encountered hardness from K1 to T3 at Devecser (5.2 km from source) suggesting that the elevated aqueous V concentration is of relatively limited extent due primarily to dilution (given the relatively consistent loading). Similar patterns are evident for Mo, with predominant transport in the dissolved phase between K1 and K3 (Figure 2). The bulk sediment analyses reports only

Table 2. Mean Composition of Digested Fluvial Sediments (n = 3) at Selected Sample Stations on the Torna Creek and Marcal River[a]

element	K1	FA	K2	K3	T1	T3	T4	S1	T5	T6	M2	*M1*	*T2*	TEL (PEL)[b]
Ca	53501	156762	107091	79138	79910	88713	82587	47909	73069	67855	62944	17083	40409	
Mg	2982	10336	16105	7111	8733	10650	8831	3674	7718	6741	6045	3859	10534	
K	737	1365	10148	5543	5476	7056	6025	2637	5239	4634	4170	8166	9235	
Na	39918	2782	6630	19391	21980	16000	19123	43224	26116	29488	32942	5350	9522	
Fe	210265	16558	37398	113480	141564	48123	30841	174425	29266	81109	80965	11142	13055	
Al	75160	20132	48407	56318	59628	54785	56910	65307	59001	60406	61571	22829	27292	
Si	27925	26544	91417	75909	65084	77470	72821	47717	66002	62180	58633	339271	54682	
As	78.5	29.9	32.3	51.9	54.3	46.2	50.8	61.3	52.8	54.9	56.3	5.8	1.7	5.9 (17)
Ba	59.8	18.6	174.7	168.4	134.3	159.1	153.9	52.0	121.7	109.2	94.3	183.7	163.9	0.7[c]
Be	9.1	0.6	1.8	4.6	5.6	1.9	1.2	7.3	1.7	3.5	3.2	0.8	<0.1	
Cd	4.0	<0.1	0.6	1.7	2.1	1.5	1.8	2.7	2.0	2.1	2.3	0.3	0.1	0.6 (3.5)
Ce	473.2	8.4	66.4	254.8	264.8	195.3	238.3	422.5	285.4	315.4	341.1	25.5	27.5	
Co	97.1	4.9	13.0	52.4	54.1	39.8	48.8	85.3	58.0	64.0	69.1	6.0	8.5	10[c]
Cr	810.7	43.6	84.4	372.6	422.6	293.2	362.8	592.8	416.3	457.3	488.8	30.3	29.2	37.3 (90)
Cu	60.3	14.9	18.4	42.6	40.5	33.8	39.0	47.6	40.1	42.2	43.3	9.3	15.1	35.7 (197)
Ga	79.3	16.6	28.2	52.9	53.4	44.8	50.4	69.0	54.7	58.0	60.6	8.9	13.0	
Li	57.5	30.1	46.6	60.5	54.9	54.0	56.5	65.3	58.6	60.1	61.4	12.7	13.6	
Mn	2565.8	182.0	443.6	1606.8	1538.7	1196.4	1447.3	2462.3	1702.0	1870.5	2011.6	292.8	420.8	400[c]
Mo	14.4	53.0	8.8	7.3	10.1	8.7	8.7	11.2	9.5	9.8	10.2	7.7	5.4	
Ni	291.7	26.8	28.3	140.7	153.5	107.5	133.9	246.0	162.5	180.8	196.4	12.5	7.6	18 (35.9)
Pb	79.8	1.8	3.5	39.6	41.0	28.0	36.2	68.1	44.1	49.5	53.9	1.3	2.6	35 (91.3)
Sr	290.2	375.7	214.9	235.0	246.7	232.2	237.9	299.1	256.4	264.5	273.3	91.5	124.3	49[c]
Ti	24848.2	1249.2	3435.1	12415.5	15073.5	5456.9	4764.7	21474.5	3721.8	9707.5	8019.3	1692.2	3665.2	
U	338.5	57.6	36.9	156.9	177.5	123.8	152.7	247.1	174.6	191.5	204.4	<0.5	2.1	
V	891.2	185.6	114.8	458.9	488.3	354.0	433.7	743.2	510.3	562.4	605.3	28.9	34.4	50[c]
Zn	173.2	29.2	58.5	104.3	112.0	91.6	102.7	132.0	108.8	114.5	118.4	26.3	26.6	123 (315)
Zr	628.9	21.2	72.2	323.1	341.4	245.5	303.3	531.8	360.2	398.4	430.2	18.4	35.1	

[a] All values in mg kg^{-1}. Reference samples M1 and T2 shown on right hand side (italics). FA: fly ash from impoundment wall, S1: floodplain deposit from Somlóvásárhely. Sb and Se below detection limits of 0.1 mg kg^{-1} [b] TEL: Threshold Effects Level; PEL: Predicted Effects Level. [c] "Background" level. All for freshwater sediments.[32]

moderate concentrations of Mo in the red mud samples (K1a−c: 11−18 mg kg^{-1}; Table 2), with peak concentrations in the fly ash itself (53 mg kg^{-1}). Whether the enrichment of Mo in K1 waters is enhanced by the dissolution of Mo-bearing phases at pH 13 in the fly ash[20] permeable reactive barrier is uncertain. At the pH values measured Mo is predicted to be predominantly present as the stable molybdate oxyanion (MoO_4^{2-})[26] in the waters of the Torna Creek. With pH changes downstream of K3, colloidal fractions subsequently dominate instream Mo loading, which levels off in the Torna before further increase in the Marcal. No significant correlations ($p > 0.05$) were apparent however for particulate Mo with any of the major elements in particulate phase (Al, Ca, Fe, Si, Ti) although attenuation by oxides and clays would be anticipated.[29]

There is a rapid transition of Al from dissolved phase (at K1) to particulate phases at T2 (Table 1). This is consistent with the decrease in pH along the north branch of the Torna Creek. Particulate Al loading shows a marked decrease from peak instantaneous loading of 1540 kg d^{-1} downstream of K3 and T1 to less than half of that at T6, suggesting significant instream attenuation via settlement of Al phases during the Torna Creek (Figure 2). After the confluence with the Marcal, loading increases again with increased stream competence. Loadings data through the Torna Creek highlight a general trend of increase in Fe, Ti, and Si loading downstream consistent with suspended solids load trends. Particulate Ca loading curves show major gains downstream of Kolontár and Devecser (T3) reflecting entrainment of both natural fines and gypsum-amended substrates with increasing stream competence. Total suspended sediment loading in the Torna Creek (Figure 2) highlights the increasing transport of particulates with transit downstream of the site reflecting diffuse inputs (e.g., runoff from red-mud-inundated land), as well as entrainment of instream sediments. This highlights the role of the Torna and upper Marcal catchment as a net exporter of red-mud-derived sediments under survey conditions.

Bulk Sediment Analyses. Table 2 presents mean bulk concentrations of major and trace elements in the fluvial sediments. Of particular note in the source samples (K1) is enrichment of As, Ce, Co, Cr, Ni, Pt, U, V, and Zn (Table 2). All are at mean concentrations slightly higher than initial reports[4] and of a similar order to sites elsewhere.[30,31] Concentrations reported at the S1 sample are similar to those reported elsewhere after the spill[4] and are consistent with the sampling location 10 km downstream from the breach. Table 2 and Figure 3 highlight a general decline in key red-mud-associated trace elements (As, Cd, Co, Cr, Ni, and V) downstream from K1, albeit with several hotspots of enrichment and some areas of preferential dilution. Low

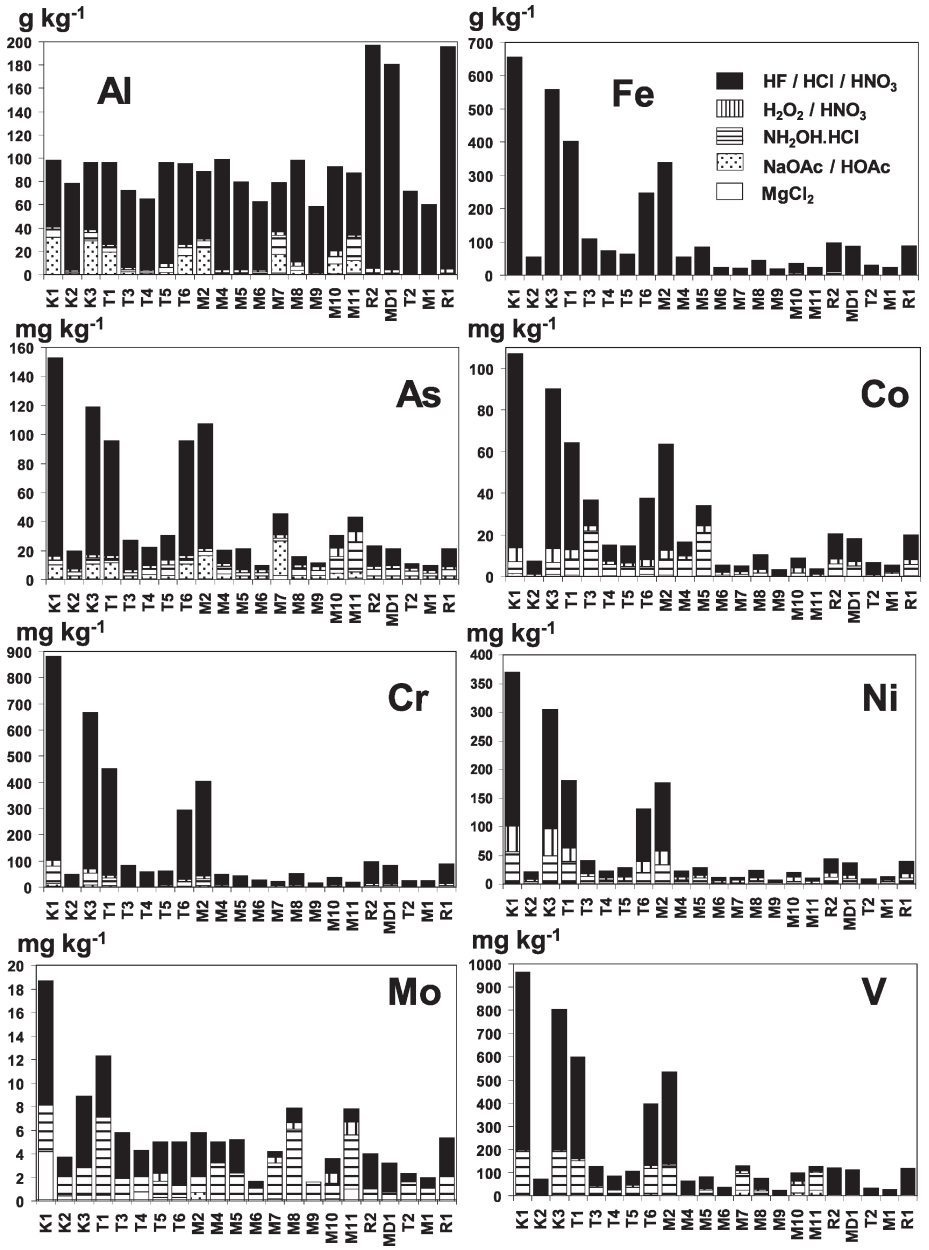

Figure 3. Sequential extraction of selected major and trace elements in stream sediment samples in the Marcal, Rába, and Mosoni-Duna rivers.

concentrations at K2 are a likely feature of the extensive disturbance to flow paths and the ground-surface in the area close to the source that has been a focus for remedial efforts. As such, K2 sediments show enrichment of many indicators of drift deposits with elevated K and lower Al, Fe, Ti, and Ca concentrations. Moderately high concentrations of trace elements are visible at T5 and T6 relative to upstream samples on Torna Creek. This may be a feature of the reduced channelization, lower gradient, and resultant velocity in the lower reaches of Torna Creek which lends itself to deposition of finer material. In the upper reaches of the Marcal (T3-T4) trapezoidal cross sections and straight planform are likely to enhance entrainment of fine-grained spill deposits and encourage dilution of bed sediments by uncontaminated, coarser sediments. Velocity data and suspended sediment loading curves (Table 1, Figure 2) support this hypothesis.

Threshold effects levels (TEL) and predicted effects levels (PEL) are widely used as an initial screening tool for potential freshwater sediment toxicity.[32] Values are presented in Table 2 for comparative purposes (and due caution in inferring mobility must be heeded) and highlight the limited spatial extent of samples that exceed PEL values, where prescribed. For Cr and Ni, concentrations well above PEL are apparent at K1, K3, T1, and T5−6. While no formal TEL/PEL values are established for Co and V, comparison with "background"[32] levels suggest enrichment patterns similar to those for Cr and Ni. It should also be noted that reference samples from urban settings (T2 from Ajka) show elevations of Cr, Ni, and V above respective background or TEL levels, indicative of urban/industrial provenance for Cr, Ni, and V in the sediments. Such diffuse urban sources (e.g., highways runoff, manufacturing industries)[33] may also account for the slight enrichment of Co, Cr, Cu, Ni, and Zn in urban reaches

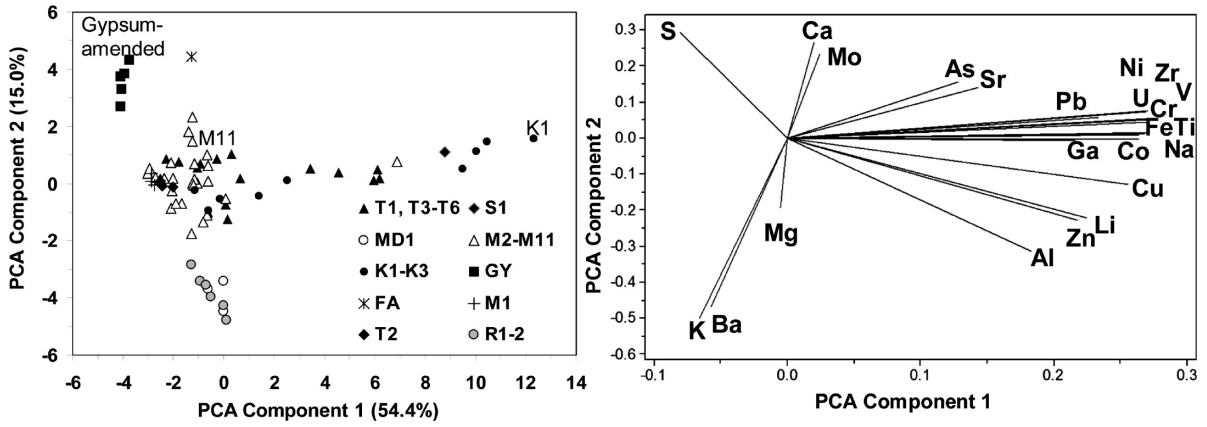

Figure 4. PCA of total fluvial sediment elemental concentrations in the studied rivers. Figures show PCA biplot by site (left image) and with eigenvectors for analyzed elements (right image).

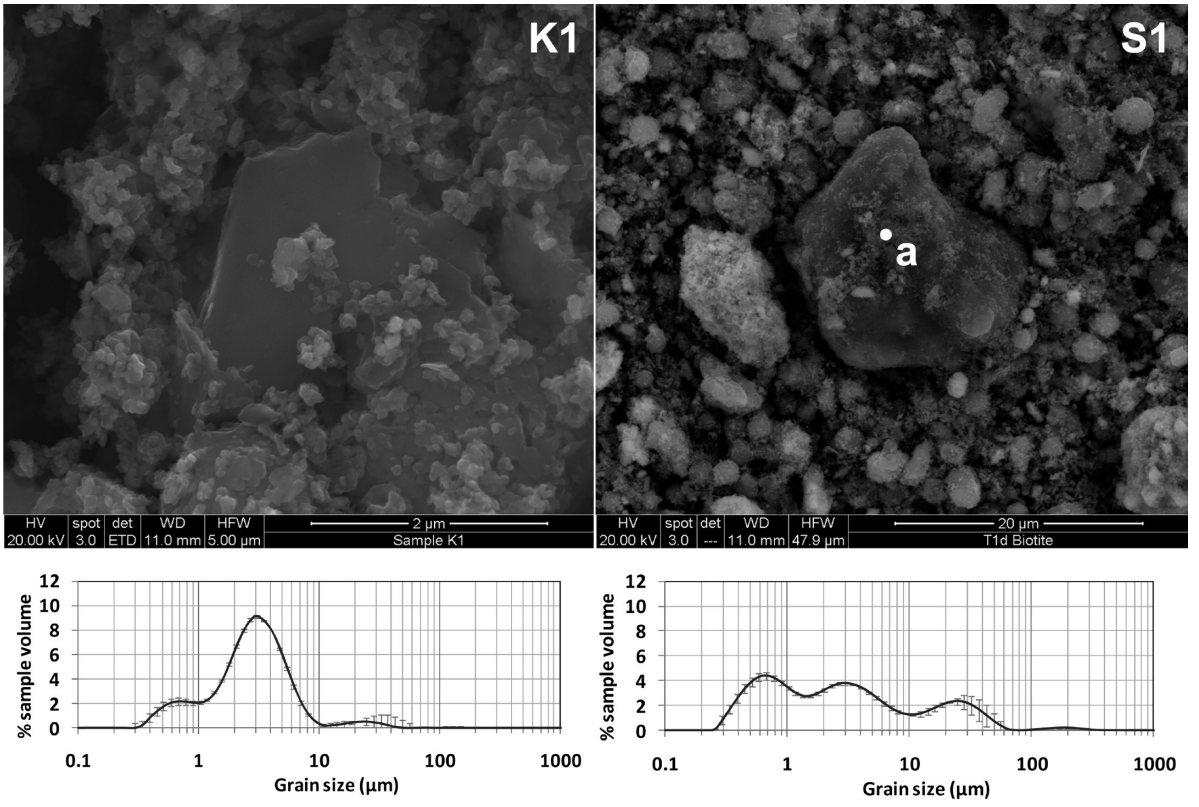

Figure 5. SEM and particle size distribution of samples K1 (source material) and S1 (transported red mud). EDS spectra for point "a" in S1.

of the Rába and Mosoni-Duna (samples R2 and MD1, Table 2). Cd samples only show significant enrichment above PEL values at site K1. Arsenic enrichment is apparent in source samples and on the Marcal at downstream stations M5 and M9 (Figure 3).

PCA analysis (Figure 4) highlights the key indicators of the red mud in the fluvial sediments and shows the mixing gradient with progression through the Torna Creek, Marcal, Rába, and Mosoni-Duna Rivers. Reference sediments (R1, T2, M1) are indicated by elevated Ba, Mg, and K relative to red-mud-contaminated sediments and indicative of lithogeneous weathering (dolomites and drift deposits[1]). PCA axis 1 shows the rapid dilution of red mud from K1 through Torna Creek, with occasional red-mud-enriched samples from the upper Marcal (M2). The second axis is characterized by the Ca-rich, gypsum-amended substrates in the lower Marcal (M11), which plots close to the fly ash sample from the dam wall given similar Ca content. Gypsum dosing of stream waters took place from Kolontár to Rábaszentmihály (Figure 1) at bridge crossings and stream access points to neutralize waters.[6]

Sequential extraction data (Figure 3) show the majority of potential contaminants in the HF/aqua-regia step. This supports interpretation of previous site data with regard to the relatively limited potential bioavailability of many trace elements.[4] High Al concentrations in the residual fraction are apparent in both undisturbed and impacted samples. Enrichment of Al in the

NaOAc and $NH_2OH \cdot HCl$ steps is apparent in source samples and suggests reasonable quantities of Al that could be transformed in suitable redox settings. Although significant inventories of Fe are associated with the $NH_2OH \cdot HCl$ step (800−3300 mg kg^{-1}), they represent only a fraction of the total Fe concentration, which is largely present as stable, well-crystallized, residual phases, such as hemeatite which is usually extracted in step 5.[5,34] Cr, Co, and Ni show broadly similar patterns with residual phases predominant, similar to patterns reported at other sites.[31] H_2O_2 and $NH_2OH \cdot HCl$ extracts contain increasing concentrations of Ni and Co downstream, while a small number of the heavily red-mud-impacted sediments (e.g., K3, T1, T6, M1) report moderate Cr inventories in weakly extractable phases such as amorphous Fe/Mn oxides and carbonates. For the more mobile elements in the aqueous phase (As, Mo, and V), greater proportions are found in nonresidual phases in transported samples in the lower Torna Creek and upper Marcal. A significant portion of V is associated with the $NH_2OH \cdot HCl$ extraction (16−60%) in samples downstream of source areas, while between 22 and 77% of Mo is associated with this fraction, suggesting the importance of oxides in attenuation of Mo and V. The importance of residual phases declines for As from source material (90%) with progress downstream (minimum of 24% at M11). Concentrations of As in the NaOAc and $NH_2OH \cdot HCl$ extraction phases reach up to 26 mg kg^{-1} at M7. These patterns for As, Mo, and V are likely to reflect instream attenuation processes (e.g., sorption to readily extractable Fe, Al oxides, and carbonate phases) during transit through the system, through which dissolved loads typically decline (Figure 2).

SEM and Particle Size Analysis. SEM analysis (Figure 5) of source material (sample K1) highlights predominant fine grained material (<4 μm in diameter) which follows a bimodal distribution comprising (1) larger, plate-like particles (diameter typically 1−6 μm), and (2) finer, more rounded particles of diameter 50−100 nm typically forming as aggregates up to 1 μm in size. The former are rich in Al, Si, and Na with significant Ca, S, Fe, and Ti (Supporting Information), consistent with cancrinite which has been identified elsewhere in samples from the site.[5] EDS spectra from the finer fractions shows consistent enrichment with Fe and O indicative of iron oxide phases (e.g., hematite) being largely hosted in these smaller particles. These nanoparticulate aggregates are likely to be driving the observed pattern of increasing suspended solid loading through the Torna Creek and Marcal River and are likely to be readily entrained even under low velocities. Analysis of transported floodplain samples (S1) shows an additional group of particles 10−40 μm in diameter indicative of entrainment of uncontaminated surface sediments (hence dilution of total concentrations at S1) in the downstream floodplain deposits (Figure 5).

Implications for System Recovery. The particularly fine-grained nature of the contaminant-bearing phases in red mud is in contrast to most river systems impacted by accidental contaminant release. Most examples of tailings failure concern metalliferous, acidic, and/or cyanide-rich materials, where sediment-borne contaminants are concentrated in fractions of the order of 10−500 μm[35] and the signal of metal contamination remains in the river system several years after the spill.[36] The data from this study suggest that within-channel storage of large inventories of red mud appears to be relatively limited in extent. Even where moderately high concentrations of trace elements (e.g., As, Cr, V) are reported, they are predominantly associated with residual phases suggesting limited potential mobility in the environment. At some depositional hotspots, association of As, Cr, and V with weak acid and oxalate extractable phases gives scope for some future mobility and should be the focus for longer-term study. Given the volume of material that was released from the impoundment and the relatively low gradient of the river system downstream of Ajka (mean gradient of 0.93 m km^{-1}), the rapid dilution of sediment-borne contaminants is encouraging and likely to reflect the preferential transport out of the system of the <10 μm fractions that characterize the released material.

■ ASSOCIATED CONTENT

Supporting Information. Detailed methods, EDS spectra, contaminant correlation, and mineral phase data.This material is available free of charge via the Internet at http://pubs.acs.org.

■ AUTHOR INFORMATION

Corresponding Author

*Tel: +44(0)1723357292; fax: +44(0)1723370815; e-mail: W.Mayes@hull.ac.uk.

■ ACKNOWLEDGMENT

This work was funded by the UK Natural Environment Research Council (grant NE/I019468/1). We are indebted to Bob Knight (University of Hull), Jane Davis (Newcastle University), Eric Condliffe and Gareth Keevil (both University of Leeds) for analyses. We also thank Mária Tolner, Ermese Vaszita (Budapest University of Technology and Economics) for field support; Gyozo Jordan (Geological Institute of Hungary), Kovacs Laszlo and István Csonki (Central Danubian Water and Environment Authority) for site information; György István Tóth for flow data and Krisztina Kocsis (British Embassy) for facilitating site access.

■ REFERENCES

(1) Reeves, H. J.; Wealthall, G.; Younger, P. L. Advisory visit to the bauxite processing tailings dam near Ajka, Vesprém County, western Hungary; British Geological Survey, Keyworth, UK, 2011; Open Report OR/11/006.

(2) Cairns, J.; Dickson, K. L.; Crossman, J. S. The biological recovery of the Clinch River following a fly ash pond spill. In *25th Industrial Waste Conference Proceedings*; Purdue University, West Lafayette, Indiana, 1972; pp182−192.

(3) Younger, P. L.; Banwart, S. A.; Hedin, R. S. *Mine Water: Hydrology, Pollution, Remediation*; Kluwer Academic Publishers, Holland, 2002.

(4) Ruyters, S.; Mertens, J.; Vassilieva, E.; Dehandschutter, B.; Poffijn, A.; Smolders, E. The red mud accident in Ajka (Hungary): Plant toxicity and trace metal bioavailability in red mud contaminated soil. *Environ. Sci. Technol.* **2011**, *45*, 1616–1622.

(5) Gelencsér, A.; Kováts, N.; Turóoczi, B.; Rostási, Á.; Hoffer, A.; Imre, K.; Nyirő-Kósa, I.; Csákberényi-Malasics, D.; Tóth, Á.; Czitrovsky, A.; Nagy, A.; Nagy, S.; Ács, A.; Kovács, A.; Ferincz, Á.; Hartyáni, Z.; Pósfai, M. The red mud accident in Ajka (Hungary): Characterization and potential health effects of fugitive dust. *Environ. Sci. Technol.* **2011**, *45*, 1608–1615.

(6) Gruiz, K. *Environmental Information: The red mud catastrophe in Hungary*. http://enfo.agt.bme.hu/drupal/en/gallery/8081 2010.

(7) Power, G.; Gräfe, M.; Klauber, C. *Review of Current Bauxite Residue Management, Disposal and Storage: Practices, Engineering and Science*; CSIRO Document DMR-3608, 2009.

(8) Palmer, S. J.; Frost, R. L.; Nguyen, T. Hydrotalcites and their role in coordination of anions in Bayer liquors: anion binding in layered double hydroxides. *Coord. Chem. Rev.* **2009**, *253*, 250–267.

(9) Somlai, J.; Jobbágy, V.; Kovács, J.; Tarján, S.; Kovács, T. Radiological aspects of the usability of red mud as building material additive. *J. Hazard. Mater.* **2008**, *150*, 541–545.

(10) Courtney, R. G.; Timpson, J. P. Reclamation of fine fraction bauxite processing residue (red mud) amended with coarse fraction residue and gypsum. *Water, Soil Air Pollut.* **2005**, *164*, 91–102.

(11) Zijlstra, J. J. P.; Dess, R.; Peretti, R.; Zucca., A. Treatment of percolate from metal sulphide mine tailings with a permeable reactive barrier of transformed red mud. *Water Environ. Res.* **2010**, *82*, 319–327.

(12) Feigl, V.; Uzinger, N.; Gruiz, K. Chemical stabilisation of toxic metals in soil microcosms. *Land Contam. Reclam.* **2009**, *17*, 485–496.

(13) Munro, L. D.; Clark, M. W.; McConchie., D. A Bauxsol^{TM}-based permeable reactive barrier for the treatment of acid rock drainage. *Mine Water Environ.* **2004**, *23*, 183–194.

(14) Khaitan, S.; Dzombak, D. A.; Lowry, G. V. Neutralization of bauxite residue with acidic fly ash. *Environ. Eng. Sci.* **2009**, *26*, 431–440.

(15) Czop, M.; Motyka, J.; Sracek, C; Szuwarzynski, O. Geochemistry of the hyperalkaline Gorka Pit Lake (pH > 13) in the Chrzanow Region, Southern Poland. *Water, Air Soil Pollut.* **2011**, *214*, 423–434.

(16) Wilkie, M. P.; Wood, C. M. The adaptations of fish to extremely alkaline environments. *Comp. Biochem. Physiol.* **1996**, *113B*, 665–673.

(17) Langmuir, D. *Aqueous Environmental Geochemistry*; Prentice-Hall: Upper Saddle River, NJ, 1997.

(18) Mayes, W. M.; Younger, P. L.; Aumônier, J. Hydrogeochemistry of alkaline steel slag leachates in the UK. *Water, Air Soil Pollut.* **2008**, *195*, 35–50.

(19) Stewart, D. I.; Burke, I. T.; Hughes-Berry, D. V.; Whittleston, R. A. Microbially-mediated chromate reduction in soil contaminated by highly alkaline leachate from chromium containing waste. *Ecol. Eng.* **2010**, *36*, 211–221.

(20) Cornelis, G.; Johnson, C. A.; Van Gerven, T.; Vandecasteele, C. Leaching mechanisms of oxyanionic metalloid and metal species in alkaline solid wastes: a review. *Appl. Geochem.* **2008**, *23*, 955–976.

(21) USEPA. *Microwave assisted acid digestion of siliceous and organically based matrices*; USEPA Method 2052; Washinton, DC, 1996

(22) Rauret, G.; Rubio, R.; Lopez-Sanchez, J. F. Optimization of Tessier Procedure for Metal Solid Speciation in river sediments. *Int. J. Environ. Anal. Chem.* **1989**, *36*, 69–83.

(23) Fällman, A.-M. Leaching of chromium and barium from steel slag in laboratory and field tests — a solubility controlled process? *Waste Manage.* **2000**, *20*, 149–154.

(24) Gupta, S. K.; Chen, K. Y. Arsenic removal by adsorption. *J. Water Pollut. Control Fed.* **1978**, *50*, 493–506.

(25) Dzombak, D. A.; Morel, F. M. M. *Surface Complexation Modelling: Hydrous Ferric Oxide*; Wiley-Interscience: New York, 1990.

(26) Takeno, N. *Atlas of Eh-pH Diagrams: Intercomparison of Thermodynamic Databases*; Geological Survey of Japan, Open File Report no. 149, 2005.

(27) Naeem, A.; Westerhoff, P.; Mustafa, S. Vanadium removal by metal (hydr)oxide adsorbents. *Water Res.* **2007**, *41*, 1596–1602.

(28) Wällstedt, T.; Björkvald, L.; Gustafsson, J. P. Increasing concentrations of arsenic and vanadium in (southern) Swedish streams. *Appl. Geochem.* **2010**, *25*, 1162–1175.

(29) Goldberg, S.; Forster, H. S.; Godfrey, C. L. Molybdenum adsorption on oxides, clay minerals and soils. *Soil Sci. Soc. Am. J.* **1996**, *60*, 425–432.

(30) Khaitan, S.; Dzombak, D. A.; Lowry, G. V. Chemistry and acid neutralization capacity of bauxite residue. *Environ. Eng. Sci.* **2009**, *26*, 873–881.

(31) Ghosh, I.; Guha, S.; Balasubramaniam, R; Kumar, A. V. R. Leaching of metals from fresh and sintered red mud. *J. Hazard. Mater.* **2011**, *185*, 662–668.

(32) Buchman, M. F. *NOAA Screening Quick Reference Tables*; NOAA HAZMAT Report 99-1; Coastal Protection and Restoration Division, National Oceanic and Atmospheric Administration: Seattle, WA, 1999; 12 pp.

(33) Westerlund, C.; Viklander, M.; Bäckström, M. Seasonal variations in road runoff quality in Luleå, Sweden. *Water Sci. Technol.* **2003**, *48*, 93–101.

(34) Xiao-Quan, S; Bin, C. Evaluation of sequential extraction for speciation of trace metals in model soil containing natural minerals and humic acid. *Anal. Chem.* **1993**, *65*, 802–807.

(35) Hudson-Edwards, K. A.; Macklin, M. G.; Jamieson, H. E.; Brewer, P. A.; Coulthard, T. J.; Howard, A. J.; Turner, J. N. The impact of tailings dam spills and clean-up operations on sediment and water quality in river systems: the Ríos Agrio—Guadiamar, Aznalcóllar, Spain. *Appl. Geochem.* **2003**, *18*, 221–239.

(36) Macklin, M. G.; Brewer, P. A.; Balteanu, D.; Coulthard, T. J.; Driga, B.; Howard, A. J.; Zaharia, S. The long term fate and environmental significance of contaminant metals released by the January and March 2000 mining tailings dam failures in Maramures County, upper Tisa Basin, Romania. *Appl. Geochem.* **2003**, *18*, 241–257.